



# Molybdenum disulfide-Zirconium dioxide composite with enhance supercapacitance performance

Razan NADHIM SHAKER<sup>1</sup>, Sami MOHAMMED<sup>2,\*</sup> and Yousra Ali ABDULSAYED<sup>3</sup>

<sup>1</sup> Department of Dentistry, Al-Noor University College, Nineveh, 10008, Iraq

<sup>2</sup> Medical technical college, Al-Farahidi University, Baghdad, 00965, Iraq

<sup>3</sup> Department of optical techniques, Al-Zahrawi University College, Karbala, 56001, Iraq

\*Corresponding author e-mail: ahkaob4@gmail.com

## Received date:

16 July 2023

## Revised date

14 November 2023

## Accepted date:

14 November 2023

## Keywords:

Molybdenum disulfide;  
Zirconium dioxide;  
Composite;  
Supercapacitor

## Abstract

As a supercapacitor active material, molybdenum disulfide (MoS<sub>2</sub>) layer offers good conductivity, large surface area, and electrochemical stability. In practice, however, its capacitance is low in comparison to other materials. This work synthesized MoS<sub>2</sub>-zirconium dioxide (ZrO<sub>2</sub>) composite in a simple, high-throughput way to test it as a supercapacitor active layer. During the tests, the composite shows a gravimetric capacitance of 500.0 F.g<sup>-1</sup>, while MoS<sub>2</sub> and ZrO<sub>2</sub> have capacitances of 265.12 and 152.43, respectively. The increase in capacitance of composite stems from the synergistic effect between ZrO<sub>2</sub>'s pseudocapacitor behavior and MoS<sub>2</sub>'s electric double layer capacitance (EDLC). Moreover, the composite has a discharge time of ~ 406 s at a current density of 1 A.g<sup>-1</sup>, which is much longer compared to MoS<sub>2</sub> and ZrO<sub>2</sub>. The stability test of the composite also shows that it maintains 93% of its initial capacitance after 2000 charge/discharge cycles.

## 1. Introduction

In the last decade, two-dimensional (2D) materials have become widely used materials in the fields of electronics, energy, and optics because they have shown unique adjustable properties [1]. Graphene is the first known atomic layer. But today, the number of 2D materials is much more than graphene, which covers almost all physical and chemical properties [2]. Among various 2D materials, the family of TMDs, which have the MX<sub>2</sub> structure (M = transition metal atom and X = halogen atoms), show more outstanding properties than other 2D materials [3]. In particular, molybdenum disulfide (MoS<sub>2</sub>) is one of the famous 2D materials of this family [4]. MoS<sub>2</sub> in its monoatomic state has different properties from its bulk state, which is very promising in the fields of energy, electrochemical and optoelectronics [4]. Due to its chemical stability and electronic transport capability, MoS<sub>2</sub> is highly favored for energy storage applications as supercapacitors [5]. In fact, the large surface area of MoS<sub>2</sub> layers increases the ion-electrode surface interaction, which has a significant effect on improving the performance of supercapacitors. Despite all these advantages, the capacitance of MoS<sub>2</sub> is still low compared to other active materials and needs a solution. As a solution to the problem, MoS<sub>2</sub>-based composites have been introduced as the active layer in supercapacitors. These composites can be composed of the combination of MoS<sub>2</sub> with carbon layers (such as graphene, and carbon nanotubes), metal oxides (such as copper oxide, and nickel oxide), or even polymers (such as PANI

[6-8]. The result is that due to the emergence of synergistic properties, the performance of supercapacitors will be greatly improved.

There are various methods to produce MoS<sub>2</sub> layers, but among them, chemical exfoliation is more effective because it leads to easy, cheap, mass production of MoS<sub>2</sub> layers, which is ideal for fabricating active layers in supercapacitors [9].

In this work, layers of MoS<sub>2</sub> were prepared through exfoliation of bulk MoS<sub>2</sub> in IPA solution using tip-sonication. The resulting solution was deposited on the FTO substrate and tested as the working electrode of the supercapacitor. In order to increase the performance of the supercapacitor, zirconium oxide (ZrO<sub>2</sub>) nanoparticles were synthesized by the hydrothermal method and added to MoS<sub>2</sub> layers to improve the energy storage ability of the electrode through the redox electrochemical process. The results show that by adding ZrO<sub>2</sub>, the electrode capacitance increases 88.6% compared to the individual MoS<sub>2</sub> electrode. The introduced composite not only has an easy, cheap, fast and safe manufacturing process compared to other reports, but also increases the MoS<sub>2</sub> capacitance significantly.

## 2. Experimental

### 2.1 Materials

Bulk molybdenum disulfide (99% purity), and Isopropyl alcohol (IPA) were supplied from Sigma-Aldrich. Sodium sulfate (Na<sub>2</sub>SO<sub>4</sub>),

zirconyl chloride octahydrate ( $ZrOCl_2 \cdot 8H_2O$ ), and ammonium hydroxide ( $NH_4OH$ ) were purchased from Merck.

## 2.2 Characterization

Hitachi-S4160 scanning electron microscopy was used to obtain FE-SEM images of the structures. CM30m Philips TEM system was employed to take the TEM image of the  $MoS_2$  layers. Raman Senterra was used to measure the Raman spectra of  $MoS_2$  in bulk and layer forms. X-ray diffraction (XRD) was done by PANalytical (XPert PRO MPD,  $Cu K\alpha 1$ ,  $\lambda = 1.5406 \text{ \AA}$ ). Supercapacitor tests were performed in a three-electrode system with  $Ag/AgCl$  as a reference electrode and Pt as a counter electrode. 1 M  $Na_2SO_4$  solution was also used as an electrolyte. An electrochemical workstation IM6 (Zahner IM6) was employed to obtain the EIS results.

## 2.3 Exfoliation of $MoS_2$

Bulk  $MoS_2$  powder with an amount of 5 mg was mixed with 30 mL of IPA through a magnetic stirrer for 15 min. Then, the resulting solution was subjected to 200 W tip-sonication for 60 min, while it was placed in a water-ice bath to remain its temperature at  $0^\circ C$ . Then the dispersion was centrifuged for 15 min at 2000 rpm and 3/4 of its upper part was collected for fabricating the working electrode.

## 2.4 Synthesis of $ZrO_2$ nanoparticles

1 g of zirconyl chloride octahydrate powder was dissolved in 80 mL of deionized water. Then, ammonium hydroxide was added slowly until the pH reached 10 while the solution was continually stirred. The resulting solution was transferred to an autoclave container and placed at a temperature of  $200^\circ C$  for 15 h. Then, the obtained solution was centrifuged several times and washed with deionized water and acetone. The collected sediment was dried at  $100^\circ C$  and calcined at  $450^\circ C$  to convert it from amorphous to crystal form.

## 2.5 Preparation of $MoS_2$ - $ZrO_2$ composite

10 mg of  $ZrO_2$  nanoparticle powder was added to  $MoS_2$  solution in IPA solvent and subjected to bath sonication for 15 min. Then the resulting solution was deposited on the FTO substrate.

## 3. Results and discussion

$MoS_2$  layers were obtained through tip-sonication of the bulk powder in IPA solution. Electron microscopies were used to evaluate the synthesis of layers. Figure 1(a) shows the SEM image of  $MoS_2$  layers that completely cover the substrate. The complete coverage of the substrate indicates that this method is suitable for fabricating the working electrode of the supercapacitor. Figure 1(b) shows the transmission electron microscopy image of  $MoS_2$  layers. The transparency of the layers indicates their low thickness. Also, the accumulation of layers has a proof of the mass production of layers, which is consistent with the results of Figure 1(a).

Figure 2 compares the Raman spectrum of the synthesized  $MoS_2$  layers with the bulk state. The bulk sample includes two peaks,  $E_{1g}$  and  $A_{1g}$ , which are in the range of  $381 \text{ cm}^{-1}$  and  $408 \text{ cm}^{-1}$  [10]. But these peaks have shifted to positions of  $385 \text{ cm}^{-1}$  and  $405 \text{ cm}^{-1}$  for  $MoS_2$  layers, respectively, which confirms that they are multi-layered [11].

$ZrO_2$  nanoparticles were synthesized by hydrothermal method and integrated with  $MoS_2$  to form the composite [12]. Figure 3(a) shows the SEM image of the synthesized  $ZrO_2$  nanoparticles, whose approximate size is around 70 nm to 80 nm. Figure 3(b) shows the SEM image of  $MoS_2$ - $ZrO_2$  composite. According to it, the composite is well formed and both  $MoS_2$  layers and  $ZrO_2$  nanoparticles can be seen in the image. In order to make this composite, synthesized  $ZrO_2$  nanoparticle powder was added in  $MoS_2$  dispersion and after 15 min of sonication, the obtained solution was deposited on the FTO substrate. Figure 3(c) shows the higher magnified SEM image of the composite. The corresponding EDX mapping is also provided in the Figure 3(d) which proves distribution of Mo, S, Zr, and O elements all over the sample.

XRD analysis was performed to further investigate the structure of the  $MoS_2$ ,  $ZrO_2$  and the introduced  $MoS_2$ - $ZrO_2$  composite. Figure 4-bottom shows the XRD spectrum of  $MoS_2$  layers. All the appearing peaks are related to 2H- $MoS_2$  structure where the stronger peaks are labeled in the figure [13]. The XRD spectrum of  $ZrO_2$  nanoparticle in Figure 4-center also presents peaks  $[-111]$ ,  $[111]$ ,  $[120]$ ,  $[002]$ , and  $[131]$ , which confirms the successful synthesis of this metal oxide structure [12]. The standard reference patterns of  $MoS_2$  and  $ZrO_2$  are also added to the Figure. In the XRD spectrum of the composite in Figure 4-top, the peaks of both  $MoS_2$  and  $ZrO_2$  structures are observed, which confirms that the synthesis of the composite was successful.

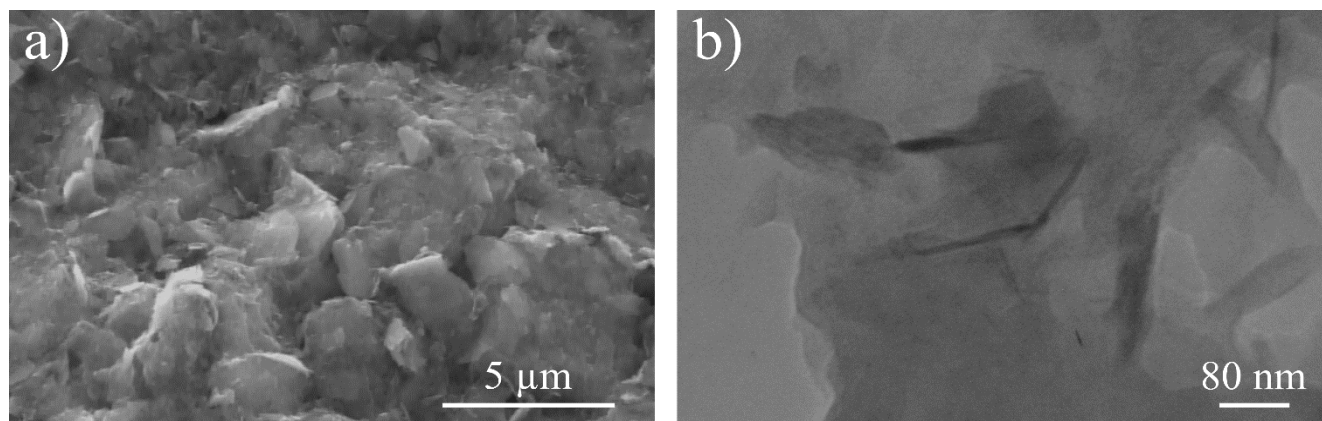


**Figure 1.** (a) SEM image of the  $MoS_2$  layers and (b) TEM image of  $MoS_2$  layers.

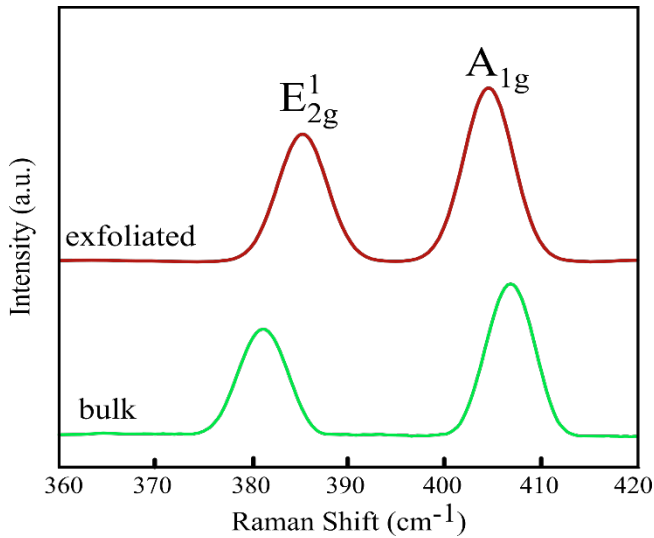
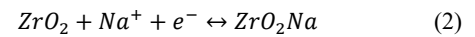
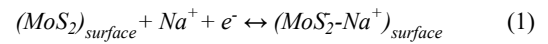


**Figure 2.** Raman spectrum of bulk and layers of MoS<sub>2</sub>.

To manufacture the working electrodes, the solution containing MoS<sub>2</sub>, ZrO<sub>2</sub> and MoS<sub>2</sub>-ZrO<sub>2</sub> was deposited on the FTO substrate and dried. To test the supercapacitor performance of all three electrodes, a three-electrode electrochemical system was used in sodium sulfate solution with 1 M. Figure 5(a-c) present the current density versus applied potential curves for MoS<sub>2</sub>, ZrO<sub>2</sub> and MoS<sub>2</sub>-ZrO<sub>2</sub> at different scan rates. Their performance is compared at a scan rate of 50 mV in the Figure 5(d). Accordingly, the MoS<sub>2</sub> curve has a rectangular shape, which refers to the behavior of its dominant electric double layer capacitance (EDLC) in energy storage [5]. For ZrO<sub>2</sub>, its current-

voltage curve has two peaks, which refers to its pseudocapacitor performance to store energy [14]. However, because the conductivity of metal oxide is lower than that of MoS<sub>2</sub>, the internal area of its curve is lower than that of MoS<sub>2</sub>. In the MoS<sub>2</sub>-ZrO<sub>2</sub> electrode, the inner area of the curve is larger than the other two electrodes, and it shows the combined EDLC and pseudocapacitor behavior. Figure 5(b) compares the performance of the MoS<sub>2</sub>-ZrO<sub>2</sub> electrode at different scan rates. As the scan rate increases, the inner area of the curves has increased, but their shape remains almost the same. Figure 5(e) compares the performance of all three electrodes in terms of scan rate from 5 mV·s<sup>-1</sup> to 50 mV·s<sup>-1</sup>. At the scan rate of 5 mV·s<sup>-1</sup>, the gravimetric capacitance was calculated as 500.00, 265.12 and 152.43 F·g<sup>-1</sup> for MoS<sub>2</sub>-ZrO<sub>2</sub>, MoS<sub>2</sub> and ZrO<sub>2</sub>, respectively. The significant increase in the capacitance value of the composite is due to the synergistic effects and occurrence of the EDLC and pseudocapacitance behavior of the composite electrode. Equations (1-2) describe the mechanism of energy storage in MoS<sub>2</sub>-ZrO<sub>2</sub> composite as follow:



Accordingly, MoS<sub>2</sub> stores energy through the combination of non-faradic and faradic process, while ZrO<sub>2</sub> nanoparticles participates in the energy storage process by providing active sites through faradic redox reactions. Furthermore, effective charge transfer between two structures has an effective role in increasing the synergistic effect in the composite [5].

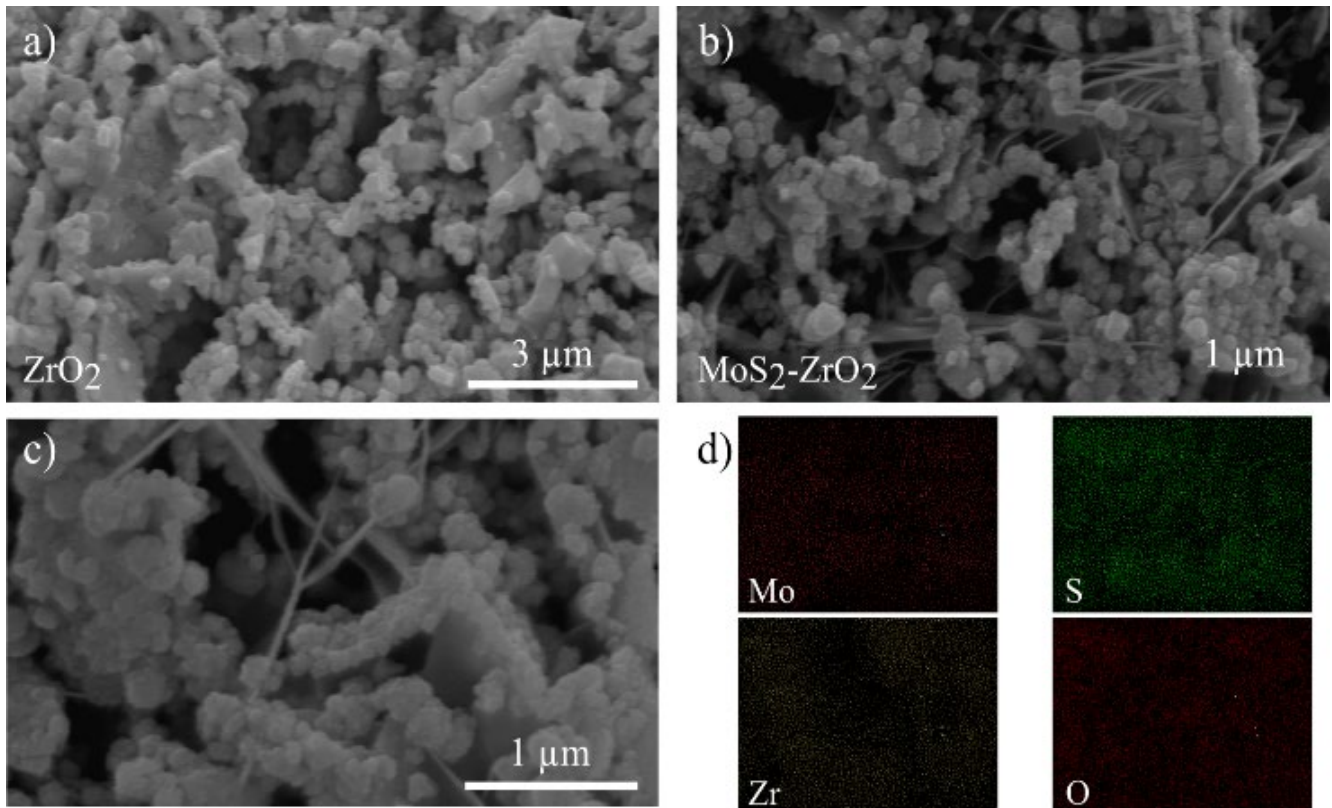


**Figure 3.** a) SEM image of ZrO<sub>2</sub> nanoparticles, and b) SEM image of MoS<sub>2</sub>-ZrO<sub>2</sub> composite. c) higher magnified SEM image of the composite with d) its EDX mapping images.

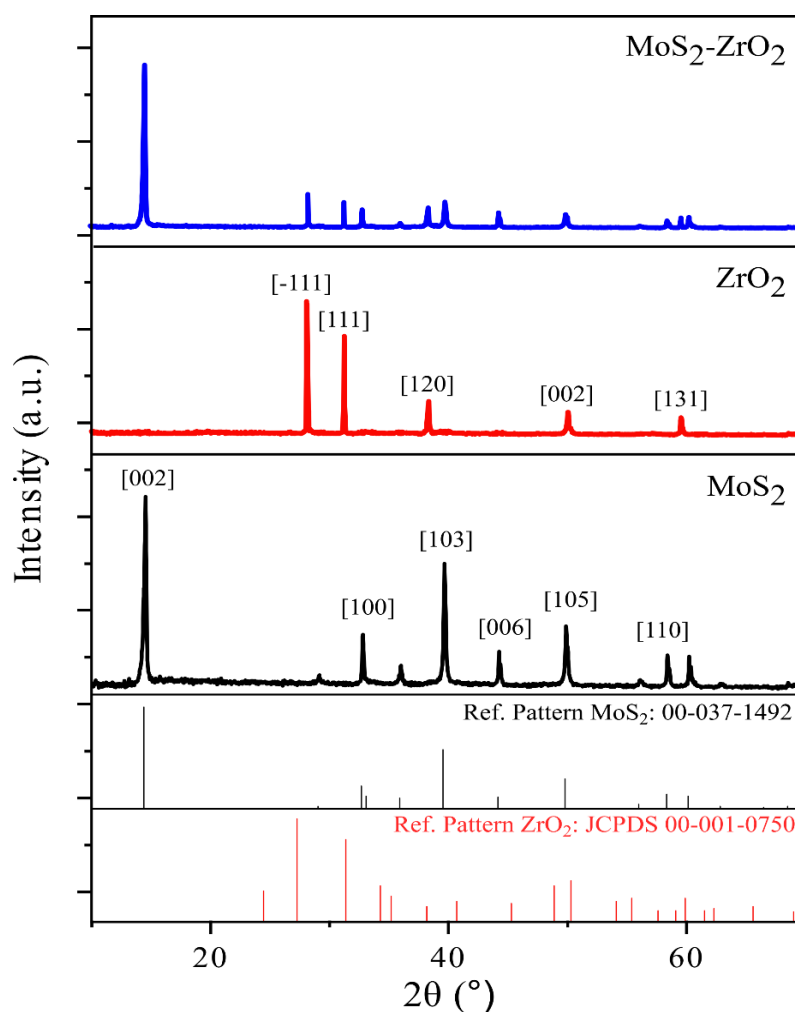


**Figure 4.** XRD spectrum of  $\text{MoS}_2$ ,  $\text{ZrO}_2$  and  $\text{MoS}_2\text{-ZrO}_2$  composite with the standard references of the  $\text{MoS}_2$  and  $\text{ZrO}_2$ .

It is also observed that the capacitance value decreases with the increase of the scan rate from  $5 \text{ mV}\cdot\text{s}^{-1}$  to  $50 \text{ mV}\cdot\text{s}^{-1}$ , since the diffusion of ions into the active layer is limited with the increase of the scan rate [5].

Galvanostatic charge/discharge (GCD) test was performed to evaluate the performance of all three  $\text{MoS}_2$ ,  $\text{ZrO}_2$  and composite electrodes. The GCD curves of the  $\text{MoS}_2\text{-ZrO}_2$  composite are depicted in Figure 6(a) at different current densities from  $1 \text{ A}\cdot\text{g}^{-1}$  to  $15 \text{ A}\cdot\text{g}^{-1}$ . Figure 6(b) shows the curves of all three electrodes at a current density of  $1 \text{ A}\cdot\text{g}^{-1}$ . According to it, the  $\text{MoS}_2\text{-ZrO}_2$  composite has the longest discharge time of about 409.05 s.  $\text{MoS}_2$  and  $\text{ZrO}_2$  each have a discharge time of 218.14 s and 128.88 s, respectively. The long discharge time of the composite shows its larger capacitance than the other two electrodes. The comparison of the GCD performance of the all electrodes are presented in Figure 6(c) where  $\text{MoS}_2\text{-ZrO}_2$  composite shows the

higher capacitance at all current densities. Figure 6 d) presents the performance of the all electrodes during 2000 charge and discharge cycles. The results indicate that the composite electrode maintains 93% of its initial capacitance while 96% and 90% of the initial capacitance of  $\text{MoS}_2$  and  $\text{ZrO}_2$  remained after 2000 cycles, respectively.

The impedance electrochemical spectroscopy (EIS) was also performed to further investigate charge transfer within the electrodes. In the Nyquist plot, the radius of the semicircular indicates the charge transfer resistance ( $R_{ct}$ ) in the sample [5]. According to the Figure 7, the  $\text{MoS}_2\text{-ZrO}_2$  electrode has a smaller radius suggesting reduced charge transfer resistance within the heterostructure in comparison to  $\text{MoS}_2$  and  $\text{ZrO}_2$  electrodes.

Table 1 summarizes the results of the  $\text{MoS}_2\text{-ZrO}_2$  composite electrode in energy storage with other  $\text{MoS}_2$ -based composites in the literature.

**Table 1.** Comparison of  $\text{MoS}_2\text{-ZrO}_2$  composite performance with other reports.

Material	Electrolyte	Potential window	Capacitance	Ref
$\text{MoS}_2\text{-ZrO}_2$	1M $\text{Na}_2\text{SO}_4$	0.0 V to 0.7 V (vs Ag/AgCl)	$500 \text{ F}\cdot\text{g}^{-1}$ at $5 \text{ mV}\cdot\text{s}^{-1}$	here
$\text{MoS}_2$	1M $\text{Li}_2\text{SO}_4$	-1 V to 0 V (vs Ag/AgCl)	$119 \text{ F}\cdot\text{g}^{-1}$ at $5 \text{ mV}\cdot\text{s}^{-1}$	[15]
$\text{MoS}_2\text{-MoO}_3$	1M $\text{Na}_2\text{SO}_4$	0.0 V to 0.9 V (vs Ag/AgCl)	$200 \text{ F}\cdot\text{g}^{-1}$ at $5 \text{ mV}\cdot\text{s}^{-1}$	[5]
$\text{MoS}_2/\text{MoO}_2/\text{CNT}$	1M KOH	0.0 V to 0.5 V (vs Ag/AgCl)	$228 \text{ F}\cdot\text{g}^{-1}$ at $0.5 \text{ A}\cdot\text{g}^{-1}$	[16]
Graphene/ $\text{ZrO}_2$	1M $\text{H}_2\text{SO}_4$	0.0 V to 0.8 V (vs Ag/AgCl)	$922 \text{ F}\cdot\text{g}^{-1}$ at $2 \text{ mV}\cdot\text{s}^{-1}$	[17]

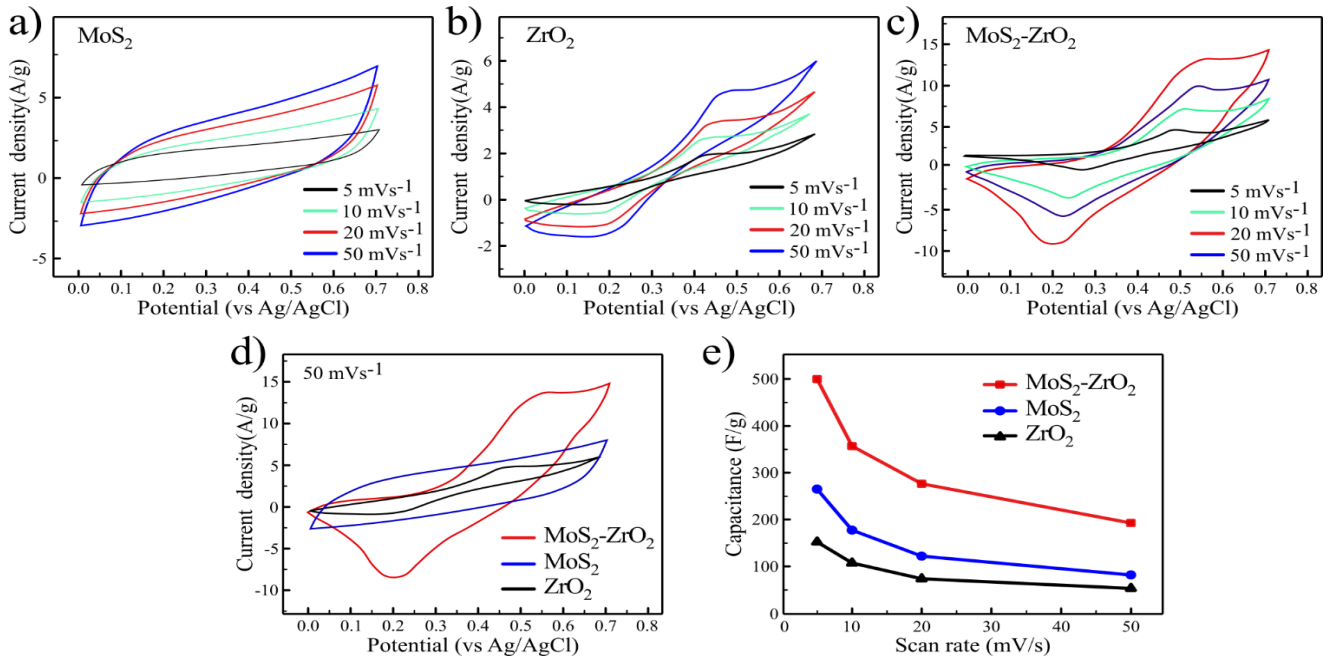


**Figure 5.** Current density-potential curves of the a) MoS<sub>2</sub>, b) ZrO<sub>2</sub>, and MoS<sub>2</sub>-ZrO<sub>2</sub> electrodes at different scan rates. d) comparison of the current density-potential of the all electrodes at a scan rate of 50 mV/s. e) gravimetric capacitance as a function of scan rate for all fabricated electrodes.

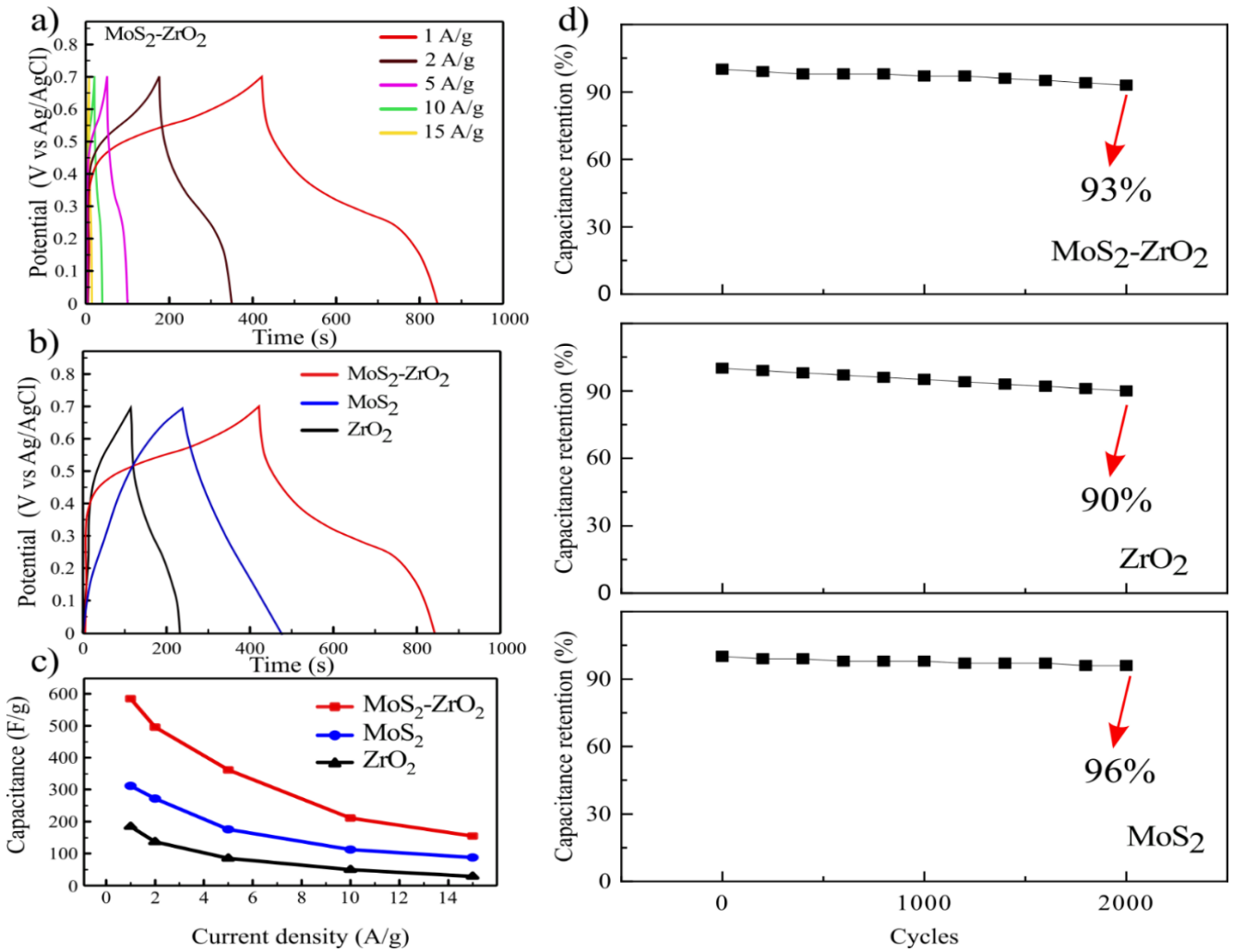


**Figure 6.** GCD test of the (a) MoS<sub>2</sub>-ZrO<sub>2</sub> at different current densities, (b) GCD curves of the all electrodes at a current density of 1 A.g<sup>-1</sup>. (c) comparison of the calculated capacitance for all electrodes at different current densities, and d) Retention performance of the all electrode after 2000 cycles.

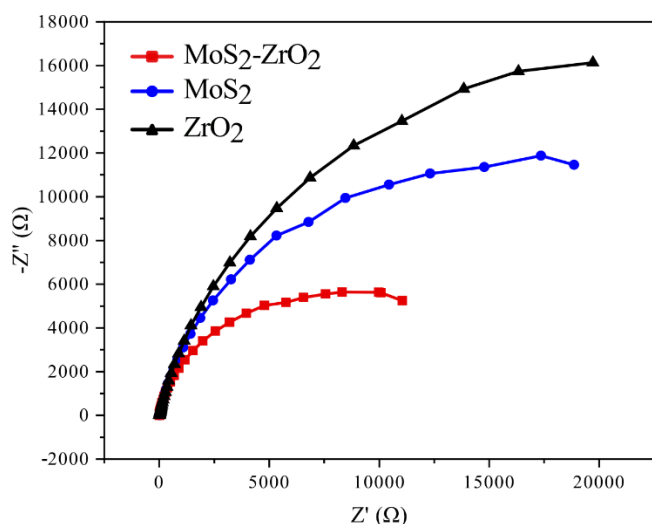


Figure 7. EIS plots of the MoS<sub>2</sub>-ZrO<sub>2</sub>, MoS<sub>2</sub>, and ZrO<sub>2</sub> electrodes.

#### 4. Conclusions

Molybdenum disulfide (MoS<sub>2</sub>) layer is promising as the active material of supercapacitors due to its large effective surface area, good conductivity and electrochemical stability. But in practice, its capacitance is low compared to other materials. In this work, MoS<sub>2</sub>-zirconium dioxide (ZrO<sub>2</sub>) composite was synthesized in a simple and high throughput way and tested as a supercapacitor active layer. The results of the tests indicate that the composite has a gravimetric capacitance of 500.0 F·g<sup>-1</sup>, while MoS<sub>2</sub> and ZrO<sub>2</sub> have a smaller capacitance of 265.12 F·g<sup>-1</sup> and 152.43 F·g<sup>-1</sup>. This increase in capacitance is due to the synergistic effect caused by the pseudocapacitor behavior of ZrO<sub>2</sub> and the electric double layer capacitance (EDLC) behavior of MoS<sub>2</sub>.

#### References

- [1] R. Bian, C. Li, Q. Liu, G. Cao, Q. Fu, P. Meng, J. Zhou, F. Liu, and Z. Liu, "Recent progress in the synthesis of novel two-dimensional van der Waals materials," *National Science Review*, vol. 9, no. 5, 2021.
- [2] F. Ghasemi, and A. Salimi, "Advances in 2d based field effect transistors as biosensing platforms: From principle to biomedical applications," *Microchemical Journal*, vol. 187, p. 108432, 2023.
- [3] M. Ali, A. M. Afzal, M. W. Iqbal, S. Mumtaz, M. Imran, F. Ashraf, A. Ur Rehman, and F. Muhammad, "2D-TMDs based electrode material for supercapacitor applications," *International Journal of Energy Research*, vol. 46, no. 15, pp. 22336-22364, 2022.
- [4] O. Samy, S. Zeng, M. D. Birowosuto, and A. El Moutaouakil, "A Review on MoS<sub>2</sub> properties, synthesis, sensing applications and challenges," *Crystals*, vol. 11, no. 4, pp. 355, 2021.
- [5] M. Rashidi, and F. Ghasemi, "Thermally oxidized MoS<sub>2</sub>-based hybrids as superior electrodes for supercapacitor and photo-electrochemical applications," *Electrochimica Acta*, vol. 435, p. 141379, 2022.
- [6] J. Dai, C. Yang, Y. Xu, X. Wang, S. Yang, D. Li, L. Luo, L. Xia, J. Li, X. Qi, A. Cabot, and L. Dai, "MoS<sub>2</sub>@Polyaniline for aqueous ammonium-ion supercapacitors," *Advanced Materials*, p. 2303732, 2023.
- [7] D. Kasinathan, P. Prabhakar, P. Muruganandam, B. R. Wiston, A. Mahalingam, and G. Sriram, "Solution processed NiO/MoS<sub>2</sub> heterostructure nanocomposite for supercapacitor electrode application," *Energies*, vol. 16, no. 1, pp. 335, 2023.
- [8] D. N. Sangeetha, M. S. Santosh, and M. Selvakumar, "Flower-like carbon doped MoS<sub>2</sub>/Activated carbon composite electrode for superior performance of supercapacitors and hydrogen evolution reactions," *Journal of Alloys and Compounds*, vol. 831, p. 154745, 2020.
- [9] F. Ghasemi, and S. Mohajerzadeh, "Sequential solvent exchange method for controlled exfoliation of MoS<sub>2</sub> Suitable for photo-transistor fabrication," *ACS Applied Materials & Interfaces*, vol. 8, no. 45, pp. 31179-31191, 2016.
- [10] J. H. Aguiar Sousa, B. S. Araújo, R. S. Ferreira, A. San-Miguel, R. S. Alencar, and A. G. Souza Filho, "Pressure tuning resonance raman scattering in monolayer, trilayer, and many-layer molybdenum disulfide," *ACS Applied Nano Materials*, vol. 5, no. 10, pp. 14464-14469, 2022.
- [11] E. Mahmoodi, M. H. Amiri, A. Salimi, R. Frisenda, E. Flores, J. R. Ares, I. J. Ferrer, A. Castellanos-Gomez, and F. Ghasemi, "Paper-based broadband flexible photodetectors with van der Waals materials," *Scientific Reports*, vol. 12, no. 1, pp. 12585, 2022.
- [12] C. V. Reddy, B. Babu, I. N. Reddy, and J. Shim, "Synthesis and characterization of pure tetragonal ZrO<sub>2</sub> nanoparticles with enhanced photocatalytic activity," *Ceramics International*, vol. 44, no. 6, pp. 6940-6948, 2018.
- [13] F. Ghasemi, and M. Hassanpour Amiri, "Facile in situ fabrication of rGO/MoS<sub>2</sub> heterostructure decorated with gold nanoparticles with enhanced photoelectrochemical performance," *Applied Surface Science*, vol. 570, p. 151228, 2021.
- [14] Y. Xiao, S. Li, C. Peng, N. Yang, S. Liu, and S. Yu, "Dual pseudocapacitive electrode/redox electrolyte systems for asymmetric supercapacitors," *Applied Surface Science*, vol. 616, p. 156552, 2023.
- [15] D. Kesavan, V. K. Mariappan, P. Pazhamalai, K. Krishnamoorthy, and S.-J. Kim, "Topochemically synthesized MoS<sub>2</sub> nanosheets: A high performance electrode for wide-temperature tolerant aqueous supercapacitors," *Journal of Colloid and Interface Science*, vol. 584, pp. 714-722, 2021.
- [16] Y. Tian, H. Du, M. Zhang, Y. Zheng, Q. Guo, H. Zhang, J. Luo, and X. Zhang, "Microwave synthesis of MoS<sub>2</sub>/MoO<sub>3</sub>@CNT nanocomposites with excellent cycling stability for supercapacitor electrodes," *Journal of Materials Chemistry C*, vol. 7, no. 31, p. 9545-9555, 2019.
- [17] S. Giri, D. Ghosh, and C. K. Das, "Growth of vertically aligned tunable polyaniline on graphene/ZrO<sub>2</sub> nanocomposites for supercapacitor energy-storage application," *Advanced Functional Materials*, vol. 24, no. 9, pp. 1312-1324, 2014.